



Universiteit
Leiden
The Netherlands

Modulation of the canonical Wnt signaling pathway in bone and cartilage

Miclea, R.L.

Citation

Miclea, R. L. (2011, November 30). *Modulation of the canonical Wnt signaling pathway in bone and cartilage*. Retrieved from <https://hdl.handle.net/1887/18153>

Version: Corrected Publisher's Version

License: [Licence agreement concerning inclusion of doctoral thesis in the Institutional Repository of the University of Leiden](#)

Downloaded from: <https://hdl.handle.net/1887/18153>

Note: To cite this publication please use the final published version (if applicable).

Chapter 6

Inhibition of Gsk3 β in cartilage induces osteoarthritic features through activation of the canonical Wnt signaling pathway

R.L. Miclea¹, M. Siebelt², L. Finos³, J.J. Goeman³, C.W. Löwik⁴, W. Oostdijk¹, H. Weinans², J.M. Wit¹, E.C. Robanus-Maandag⁵, M. Karperien⁶

¹*Department of Pediatrics, Leiden University Medical Centre (LUMC), Leiden, The Netherlands,* ²*Department of Orthopaedics, Erasmus University Medical Center, Rotterdam, The Netherlands,* ³*Department of Medical Statistics, LUMC, Leiden, The Netherlands,* ⁴*Department of Endocrinology and Metabolic Diseases, LUMC, Leiden, The Netherlands,* ⁵*Department of Human Genetics, LUMC, Leiden, The Netherlands,* ⁶*MIRA Institute for Biomedical Technology and Technical Medicine, University of Twente, Department of Tissue Regeneration, Enschede, The Netherlands*

Osteoarthritis Cartilage 2011

Inhibition of Gsk3 β in cartilage induces osteoarthritic features through activation of the canonical Wnt signaling pathway

R.L. Miclea, M. Siebelt, L. Finos, J.J. Goeman, C.W. Löwik, W. Oostdijk, H. Weinans, J.M. Wit, E.C. Robanus-Maandag, M. Karperien

ABSTRACT

In the past years, the canonical Wnt/ β -catenin signaling pathway has emerged as a critical regulator of cartilage development and homeostasis. In this pathway, glycogen synthase kinase-3 β (GSK3 β) down-regulates transduction of the canonical Wnt signal by promoting degradation of β -catenin. In this study we wanted to further investigate the role of Gsk3 β in cartilage maintenance. Therefore, we have treated chondrocytes *ex vivo* and *in vivo* with GIN, a selective GSK3 β inhibitor.

In E17.5 fetal mouse metatarsals, GIN treatment resulted in loss of expression of cartilage markers and decreased chondrocyte proliferation from day 1 onward. Late (3 days) effects of GIN included cartilage matrix degradation and increased apoptosis. Prolonged (7 days) GIN treatment resulted in resorption of the metatarsal. These changes were confirmed by microarray analysis showing a decrease in expression of typical chondrocyte markers and induction of expression of proteinases involved in cartilage matrix degradation. An intra-articular injection of GIN in rat knee joints induced nuclear accumulation of β -catenin in chondrocytes 72 hours later. Three intra-articular GIN injections with a two days interval were associated with surface fibrillation, a decrease in glycosaminoglycan expression and chondrocyte hypocellularity 6 weeks later.

These results suggest that, by down-regulating β -catenin, Gsk3 β preserves the chondrocytic phenotype, and is involved in maintenance of the cartilage extracellular matrix. Short term β -catenin upregulation in cartilage secondary to Gsk3 β inhibition may be sufficient to induce osteoarthritis-like features *in vivo*.

INTRODUCTION

Differentiated chondrocytes maintain their phenotype via synthesis of cartilage-specific extracellular matrix (ECM) molecules including collagen type II and sulfated proteoglycans, like aggrecan (1). Chondrocytes easily lose essential characteristics when they are removed from their natural environment and cultured *in vitro* or expanded for the purpose of cartilage tissue engineering (1;2). Chondrocyte dedifferentiation also occurs in the presence of retinoic acid, nitric oxide, or proinflammatory cytokines like interleukin (IL)-1 β and TNF- α , as well as in osteoarthritis (OA) (2).

We and others have shown that both constitutive up- or down-regulation of the canonical Wnt pathway negatively influences cartilage development and maintenance resulting in OA-like features. This suggests that a tight regulation of this signaling cascade is crucial throughout the chondrocyte life-cycle (3-6). In this pathway, in the absence of a Wnt signal, a destruction complex comprising Axin (Conductin) and Adenomatous polyposis coli (APC) mediates the phosphorylation of β -catenin by GSK3 β , which induces degradation of cytosolic β -catenin in the proteasome. Binding of Wnt to its transmembrane receptor Frizzled results in activation of Dishevelled. This is followed by reduction of GSK3 β activity and accumulation of cytoplasmic β -catenin. Upon its nuclear translocation, β -catenin will function as a co-factor of TCF/LEF transcription factors to induce expression of Wnt target genes (6). GSK3 β is constitutively active and, unlike many kinases that are activated following stimulus-dependent phosphorylation, it becomes inactive following phosphorylation (7). Studies reported so far indicate that Gsk3 β activity is required for both chondrocyte and osteoblast differentiation and thus for endochondral bone development (8). However, no data is available regarding the role of GSK3 β in maintenance of the chondrocytic phenotype.

To better understand the role of Gsk3 β in regulation of the chondrocyte life cycle, we inactivated this kinase *ex vivo* and *in vivo* by using 3-[9-Fluoro-2-(piperidine-1-carbonyl)-1,2,3,4-tetrahydro-[1,4]diazepino[6,7,1-hi]indol-7-yl]-4-imidazo[1,2-a]pyridin-3-yl-pyrrole-2,5-dione, a selective and potent GSK3 β inhibitor, in this manuscript further referred to as GIN (9). Our results imply that Gsk3 β activity is crucial for maintenance of the chondrocytic phenotype and for the integrity of cartilage ECM, mainly by down-regulating the canonical Wnt signaling pathway. The cartilage phenotypic changes induced by GIN bear similarities to some of the clinical features commonly observed in OA.

MATERIALS AND METHODS

KS483 cell culture, immunofluorescence for β -catenin, transient transfection assays

Routine culture of KS483 cells in T75 culture flasks (Greiner Bio-One), immunofluorescence for β -catenin and transient transfection assays were performed as previously described (10).

***Ex vivo* experiments**

The three middle metatarsals were dissected from E17.5 Swiss Albino mouse embryos. Explants isolated from different animals were randomly distributed and individually cultured in 500 μ l α -MEM (Invitrogen) medium containing 10% FCS (Invitrogen), 100 U Pen/Strep (Invitrogen) and 1% GlutaMax (Invitrogen). After an equilibration period of 48 hours, metatarsals were challenged with vehicle or GIN as described in the results section. All *ex vivo* experiments were approved by the ethical committee of the Leiden University Medical Center and complied with national laws relating to the conduct of animal experiments.

Proliferation and apoptosis assays

Chondrocyte proliferation was assessed by immunohistochemistry (IHC) for proliferating cell nuclear antigen (PCNA) according to manufacturer's protocol (Santa Cruz Biotechnology). Chondrocyte apoptosis was determined by the TUNEL reaction (Promega), as previously described (11). For statistical analysis a number of N = 3 independent samples were used and each experiment was repeated at least once.

Histology, Immunohistochemistry, In situ hybridization

Histology, IHC, and in situ hybridization (ISH) were performed as previously described (5).

Quantification of glycosaminoglycans

The glycosaminoglycan (GAG) content in N = 3 whole metatarsals per condition was quantified related to the amount of DNA using the Blyscan Sulfated GAG Assay kit (Biocolor) according to manufacturer's protocol. Experiments were repeated at least once.

Gene expression profiling

For each condition, RNA was isolated from N = 15 whole metatarsals, checked for quality, amplified and labeled as previously described (12). Labeled cRNA was further used for the hybridization to Affymetrix GeneChip[®] Mouse Genome 430A 2.0 Array according to the manufacturer's protocol. The raw and normalized data are deposited on the website of the Department of Tissue Regeneration of the Twente University Institute for Biomedical Technology (<http://tr.tnw.utwente.nl>).

Microarray data analysis

To evaluate the large number of genes and to find gene expression trends and noteworthy signaling pathways that are involved in the GIN-mediated effects, we used principal component analysis (13). Using a cut-off value of 2 for the expression fold change, a list of 316 differentially expressed genes (225 down- and 91 up-regulated) was generated and used for subsequent analysis (Table 1 and 2).

Functional annotation of the differentially expressed genes identified by the PCA analysis was performed using the DAVID bioinformatics database and the Gene Ontology (GO) terms to describe their (extra)cellular location (GO_CC), molecular functions (GO_MF), and the biological processes (GO_BP) in which they are involved (14-16). Enrichment of GO functional groups was determined to be meaningful when the number of probe sets in our list that mapped to a specific GO term was greater than 2 with a p-value ≤ 0.001 .

Validation of the microarray analysis was performed by real-time quantitative PCR as previously described (12).

***In vivo* experiments**

All *in vivo* experiments were approved by the ethical committee of the Erasmus University Medical Center and complied with national laws relating to the conduct of animal experiments. Thirteen-week-old male Wistar rats (400-450 g) were housed under standard laboratory conditions (temperature 24°C, 12-hour light-dark cycle) with food and water *ad libitum*. The animals were acclimatized to the laboratory environment for 3 weeks before the start of the experiments.

GIN treatment

In a dose-finding study (n=4), the effect of an intra-articular injection of 100 μ l GIN dissolved in PBS at concentrations of $3 \cdot 10^{-7}$ M, 10^{-6} M, $3 \cdot 10^{-6}$ M, and 10^{-5} M in the knee joint was investigated.

In a second experiment, 8 rats were injected intra-articularly at day 1, 3 and 5 with 100 μ l 10^{-5} M GIN. Four rats were injected with GIN in the left knee, the remaining 4 were injected in the right knee. Contralateral joints served as controls and were injected with vehicle. All animals were scanned using contrast-enhanced microCT (CECT) before GIN injection (t = 0) and during follow up as previously described (17). Rats were sacrificed at the times indicated in the text.

Microscopical analysis and quantification

IHC for β -catenin coupled with Alcian Blue (AB) counterstaining for GAGs was carried out as previously described (5). Quantification of the AB staining was performed using Image-Pro Plus software, version 7.0.

Statistical analysis

All values represent median and range for experiments when $N \leq 4$ and mean and 95% confidence interval (CI) when $N \geq 5$. The paired t-test, the univariate general linear model using simple contrasts and parameter estimates and one-way ANOVA were used

to assess the data, as appropriate. *P* values less than 0.05 were considered significant. Statistical analysis was performed using SPSS v16.0 (SPSS).

RESULTS

Inhibition of Gsk3 β through GIN results in activation of the canonical Wnt signaling pathway *in vitro* and *ex vivo*

We first performed transient transfection experiments in mesenchymal-like KS483 cells using the Wnt-responsive BAT-Luc reporter vector (10;18). As expected, GIN induced a dose-dependent increase in luciferase activity, with a maximum response at 10^{-7} M (Figure 1A). At higher concentrations, the luciferase activity decreased, presumably due to toxic effects (Figure 1A and data not shown). Furthermore, GIN was significantly more potent in inducing the Wnt reporter construct than LiCl, another established inhibitor of GSK3 β . Activation of the Wnt reporter construct by 10^{-7} M GIN was accompanied by β -catenin accumulation and nuclear translocation as confirmed by immunofluorescence (Figure 1B). The overall level of β -catenin was notably increased in cells treated with GIN when compared to LiCl (50 mM) or Wnt3a (50 ng/ml) (Figure 1B).

We next investigated the effect of GIN on fetal mouse metatarsals, which represent an established model for studying the chondrocyte life cycle *ex vivo* (19). After incubation for 3 days, GIN dose-dependently increased the levels of β -catenin as revealed by IHC (Figure 1C). Metatarsals treated with either 10^{-7} M or 10^{-6} M GIN displayed β -catenin staining mainly in the nuclei, indicating an efficient activation of the canonical Wnt signal. The latter concentration resulted in immunohistochemically detectable nuclear β -catenin expression in almost all chondrocytes. Strikingly, metatarsals treated with 10^{-6} M GIN displayed a much fainter AB counterstaining in comparison to controls, indicative for loss of GAGs. Additional morphological analysis revealed no evidence of cell death, cell shrinkage, picnotic nuclei, blebbing of the cytoplasm or necrosis. Subsequent experiments using the fetal mouse metatarsal *ex vivo* culture model were performed with 10^{-6} M GIN.

GIN inhibits chondrocyte proliferation and increases cartilage apoptosis

We assessed the effect of GIN on chondrocyte proliferation using IHC for PCNA. The percentage of proliferating cells was smaller in the GIN-treated group compared to controls at all time points examined (Figure 2A-E). Chondrocyte proliferation was significantly inhibited both at d1 (11.3% vs. 25.9%, $p = 0.048$) and at d3 (7.6% vs. 27.8%, $p = 0.014$). TUNEL staining in combination with histological evaluation was used to assess chondrocyte apoptosis. GIN did not have an effect on TUNEL positivity at 6h, d1 and d3 (Figure 2F-J). Only after prolonged GIN treatment (d7), TUNEL staining was significantly increased (22.9% vs. 6.0%, $p = 0.043$). At d7, TUNEL-positive cells were predominantly identified among the hypertrophic chondrocytes in controls. In contrast, TUNEL-positive cells were also observed among the resting and proliferative chondrocytes in

the GIN-treated group. Based on histological evaluation, TUNEL-positive cells underwent apoptosis.

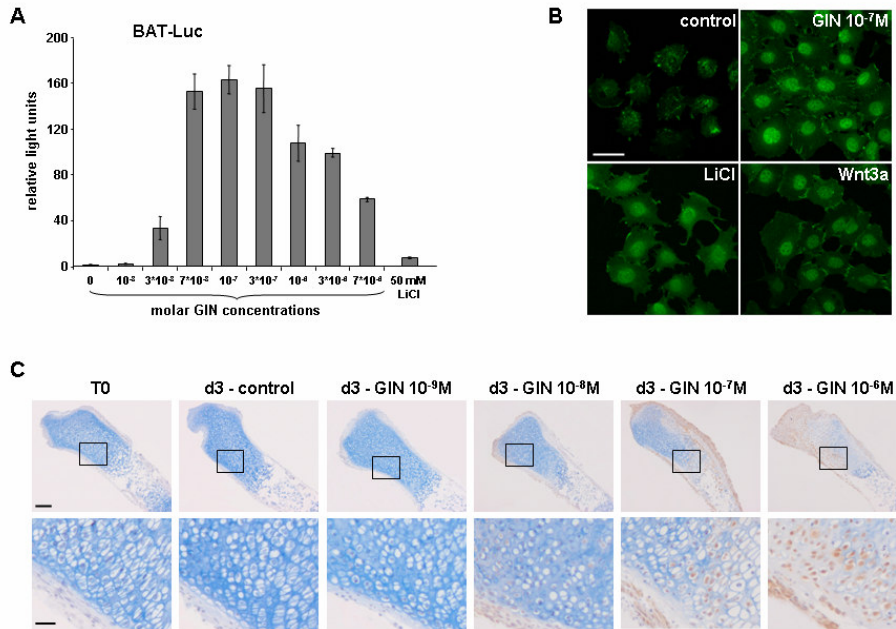


Figure 1. GIN activates the canonical Wnt signaling pathway via β -catenin. (A) GIN activated a transiently transfected Wnt reporter construct in KS483 cells dose-dependently. Values represent the mean and 95% CI (error bars) of $N = 9$ luciferase observations corrected for renilla luciferase. (B) Representative images showing the effect of GIN (10^{-7} M), LiCl (50mM) and Wnt3A (50ng/ml) on β -catenin localization in KS483 cells as revealed by immunofluorescence. Out of the three Wnt activators, GIN was most effective in stabilizing and inducing nuclear translocation of β -catenin. Scale bar = $10\mu\text{m}$. (C) Representative images showing β -catenin IHC combined with AB staining on longitudinal sections of E17.5 murine metatarsals treated for 3 days with the indicated concentrations of GIN. In this experimental set-up, 10^{-6} M GIN induces nuclear β -catenin translocation in almost all cells without any sign of toxicity. Note the progressive decrease in the intensity of the AB staining. The boxed regions in the upper row pictures are magnified in the lower row pictures. Scale bars = $100\mu\text{m}$ (upper row), $25\mu\text{m}$ (lower row).

Inhibition of Gsk3 β induces degradation of cartilage matrix and loss of the chondrocytic phenotype *ex vivo*

We investigated the effect of GIN at the cellular level by IHC analysis for β -catenin, collagen type II and X, and ISH analysis for *Col2a1* and *Col10a1*. No microscopical differences between vehicle- and GIN-treated metatarsals were observed at 6h (data not shown). β -catenin expression at the start of the experiment and in the control metatarsals at d1, d3 and d7 was restricted to the cytoplasm of a minority of perichondrial and periosteal cells (Figure 3A_i, A_{iii}, A_v). We first noticed a clear increase in the level of nuclear β -catenin after 1 day of GIN treatment (Figure 3A_{ii}). β -catenin accumulation was observed at d3 and d7 as well (Figure 3A_{iv}, A_{vi}). The level of nuclear β -catenin was

inversely correlated with the intensity of the AB counterstaining (Figure 3A-A_{vi}). GIN treatment progressively decreased the GAG content in the ECM, with a near complete loss of GAGs at d7 (Figure 3F). GIN did not have an effect on mineral deposition and ossification of the metatarsals (data not shown).

Additional microscopical analysis revealed *Col2a1* mRNA and collagen type II protein expression in the resting, proliferative and prehypertrophic chondrocytes, and their matrix, respectively, at all time points in the controls (Figure 3B, B_i, B_{iii}, B_v, C, C_i, C_{iii}, C_v). GIN treatment for 1 day resulted in a considerable inhibition of the mRNA expression of this chondrocyte marker, whereas its protein expression was not changed (Figure 3B_{ii}, C_{ii}). At d3, most of the chondrocytes in the GIN-treated metatarsals, although surrounded by a matrix rich in collagen type II, failed to express *Col2a1* (Figure 3B_{iv}, C_{iv}). At d7, neither *Col2a1* nor collagen type II expression was found in the GIN-treated metatarsals (Figure 3B_{vi}, C_{vi}).

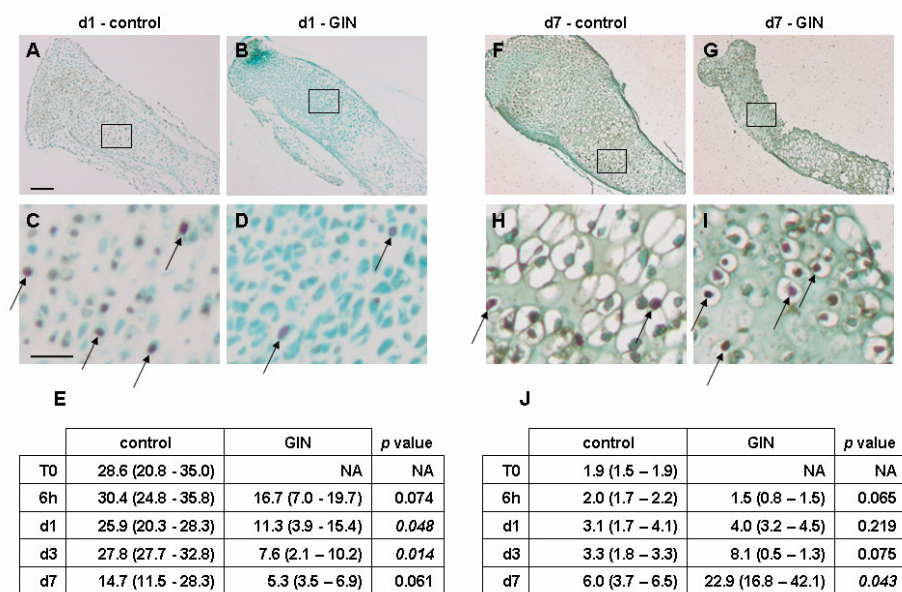


Figure 2. GIN inhibits chondrocyte proliferation and augments cartilage apoptosis. (A-D) Representative images showing PCNA IHC on metatarsals treated with vehicle (A, C) or GIN (B, D) for 1 day. Note that the number of the PCNA-positive nuclei (brown) is decreased in the GIN-treated metatarsal. (E) Quantification in N = 3 independent samples of the PCNA-positive nuclei (examples indicated by black arrows in C, D) indicates significant inhibition of chondrocyte proliferation upon GIN treatment at d1 and d3. PCNA positive cells were counted on a midsagittal tissue section. Each field contained at least 500 cells and data are expressed as median (range) % of PCNA positive cells from total number of cells. (F-I) Representative pictures of metatarsals cultured in control (F, H) or GIN-enriched (G, I) medium for 7 days after TUNEL staining. Note that the number of the TUNEL-positive nuclei (brown) is increased in the GIN-treated metatarsal. (J) Quantification in N = 3 independent samples of the TUNEL-positive nuclei (examples indicated by black arrows in H, I) indicates significantly more chondrocyte apoptosis upon prolonged GIN treatment (d7). Quantification and data expression as in (E). (C, D, H, I) High magnification pictures of the boxed regions in A, B, F, and G, respectively. Scale bars: 100 μm (A, B, F, G), 25 μm (C, D, H, I).

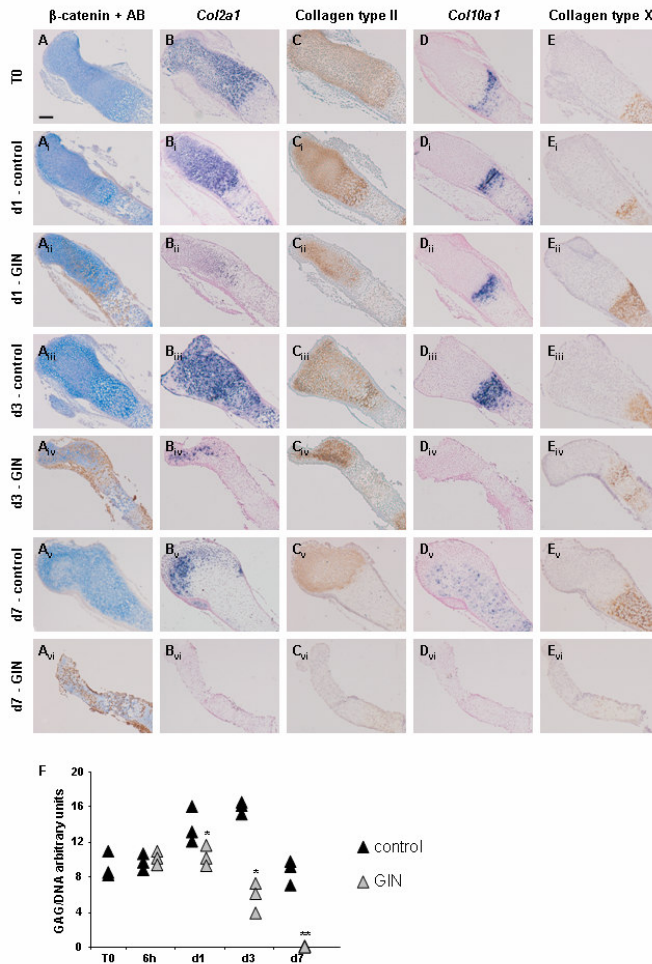


Figure 3. GIN induces loss of the chondrocytic phenotype *ex vivo*. Representative pictures of (A-A_{vi}) β -catenin immunostaining combined with AB staining, (B-B_{vi}) *Col2a1* mRNA expression, (C-C_{vi}) Collagen type II immunostaining, (D-D_{vi}) *Col10a1* mRNA expression, and (E-E_{vi}) Collagen type X immunostaining, on consecutive longitudinal sections of E17.5 mouse metatarsals (N = 3 independent samples) isolated at the indicated time points. B-catenin-positive chondrocytes lose *Col2a1* expression upon GIN treatment already at d1. Chondrocyte marker expression at the mRNA level is inhibited after 3-day-long GIN treatment. Chondrocytes exposed to GIN for 7 days fail to express specific markers at both mRNA and protein level. Scale bar: 100 μ m. (F) Quantification of GAGs corrected for DNA (N = 3 independent samples) validates the microscopical findings. *p = 0.023 (d1), *p = 0.016 (d3), **p = 0.008 (d7), all GIN vs. same time point untreated. Data are expressed in arbitrary GAG/DNA units (black triangles - controls, grey triangles - GIN treated samples).

Furthermore, control metatarsals displayed *Col10a1* and collagen type X expression in the hypertrophic zone (Figure 3D, D_i, D_{iii}, D_v, E, E_i, E_{iii}, E_v). At d1, there were no differences in the expression of this mature chondrocyte marker between the control and the GIN-treated group, neither at the mRNA nor at the protein level (Figure 3D_{ii}, E_{ii}). At d3, GIN-treated explants displayed no *Col10a1* expression, whereas collagen type X was still present in the ECM (Figure 3D_{iv}, E_{iv}). Ultimately, at d7, GIN induced a complete absence of both *Col10a1* and collagen type X (Figure 3D_{vi}, E_{vi}).

Microarray analysis confirms GIN's proteolytic effects on cartilage

To further examine the effects of GIN on gene expression patterns in the fetal mouse metatarsal model, we performed cDNA microarray analysis on mRNA isolated from GIN-treated and control explants at T0, 6h, d1 and d3. We particularly designed our microarray analysis as such since GIN-treated metatarsals at d7 showed only aggravated features of the ones observed at d3. Furthermore, the increased apoptosis at d7 would have jeopardized the specificity of the results and mainly revealed differentially expressed genes related to cell death, an indirect effect of GIN treatment.

According to GO_CC terms, the vast majority of the 316 differentially expressed genes (225 down- and 91 up-regulated) encoded proteins that are active in the ECM (Figure 4A). Classification according to GO_MF and GO_BP terms is represented in Figure 4B and 4C, respectively. The large number of up-regulated genes and the fact that they did not categorize under any GO terms related to cell death suggested that our microarray data efficiently revealed biological effects caused by GIN treatment and not by toxicity.

In consistence with the microscopical findings indicating significant cartilage matrix degradation, we found among the 91 up-regulated genes numerous transcripts encoding established proteinases: Matrix metalloproteinase 9 (*Mmp9*), *Mmp10*, *Mmp11*, and HtrA serine peptidase 1 (*Htra1*). Given the role of GSK3 β in canonical Wnt signaling, the microarray data showed evidence for a Wnt/ β -catenin signature as evidenced by the upregulation of established direct targets of the β -catenin/TCF4 complex, like Axin2 and adenomatous polyposis coli down-regulated 1 (*Apcdd1*). Microarray and pathway analysis did not reveal clear signatures of changes in other signaling pathways, such as Hedgehog and FGF. Furthermore, several cartilage ECM proteins were identified among the 225 down-regulated genes: unique cartilage matrix-associated protein (*Ucma*), matrilin 1 (*Matn1*), *Matn3*, *Matn4*, hyaluronan and proteoglycan link protein 1 (*Hapln1*), collagen, type XI, alpha 1 (*Col11a1*), epiphycan (*Epyc*), fibromodulin (*Fmod*), matrix Gla protein (*Mgp*), *Col14a1*, and (*Col9a3*). In the list of repressed genes, we also found transcripts known to encode non-cartilaginous matrix proteins like osteomodulin (*Omd*), osteoglycin (*Ogn*), microfibrillar-associated protein 4 (*Mfap4*), tenomodulin (*Tnmd*), asporin (*Aspn*), and fibulin7 (*Fbln7*), suggesting a more complex effect of the GIN treatment on the extracellular matrix.

To independently validate the results of the microarray analysis, 16 genes were selected for confirmation by quantitative real-time RT-PCR analysis. For the transcriptional analysis we therefore isolated RNA from a separate experiment that mirrored the one used to generate the microarray data. Four of these 16 genes are known to be involved in chondrocyte differentiation and cartilage maintenance (*Sox9*, *Col2a1*, *Acan*

and *Col10a1*), 4 are members of the canonical Wnt signaling pathway (*Axin1*, *Axin2*, *Gsk3b* and *Ctnnb1*), and 8 encode proteinases known to regulate maintenance and degradation of the ECM (*Mmp2*, *Mmp3*, *Mmp9*, *Mmp13*, *Adams4*, *Adams5*, *Hyal1* and *Ctsk*). We found a similar expression pattern of the analyzed genes, indicating that our microarray data specifically corresponded to actual gene expression patterns (Figure 5).

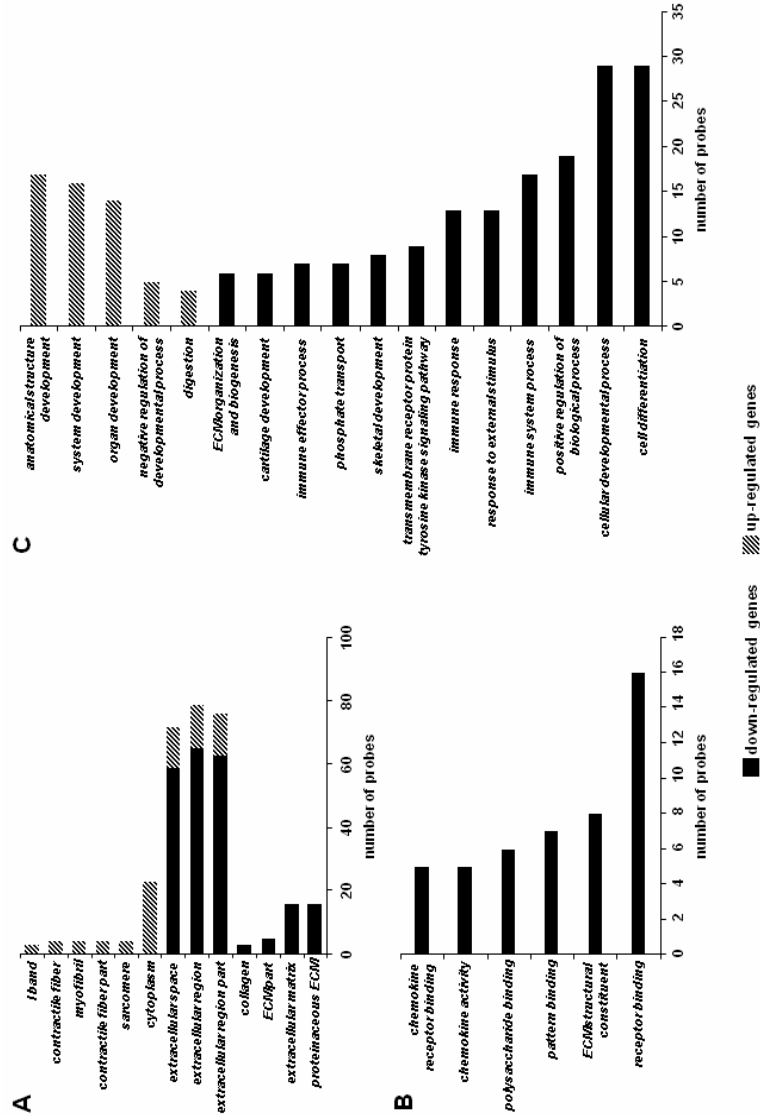


Figure 4. Functional annotation of the GIN-modulated genes according to GO terms. Functional annotation according to GO_CC (A), GO_MIF (B) and GO_BP (C) terms was used to determine the enrichment of the differentially expressed transcripts indicated by PC1.

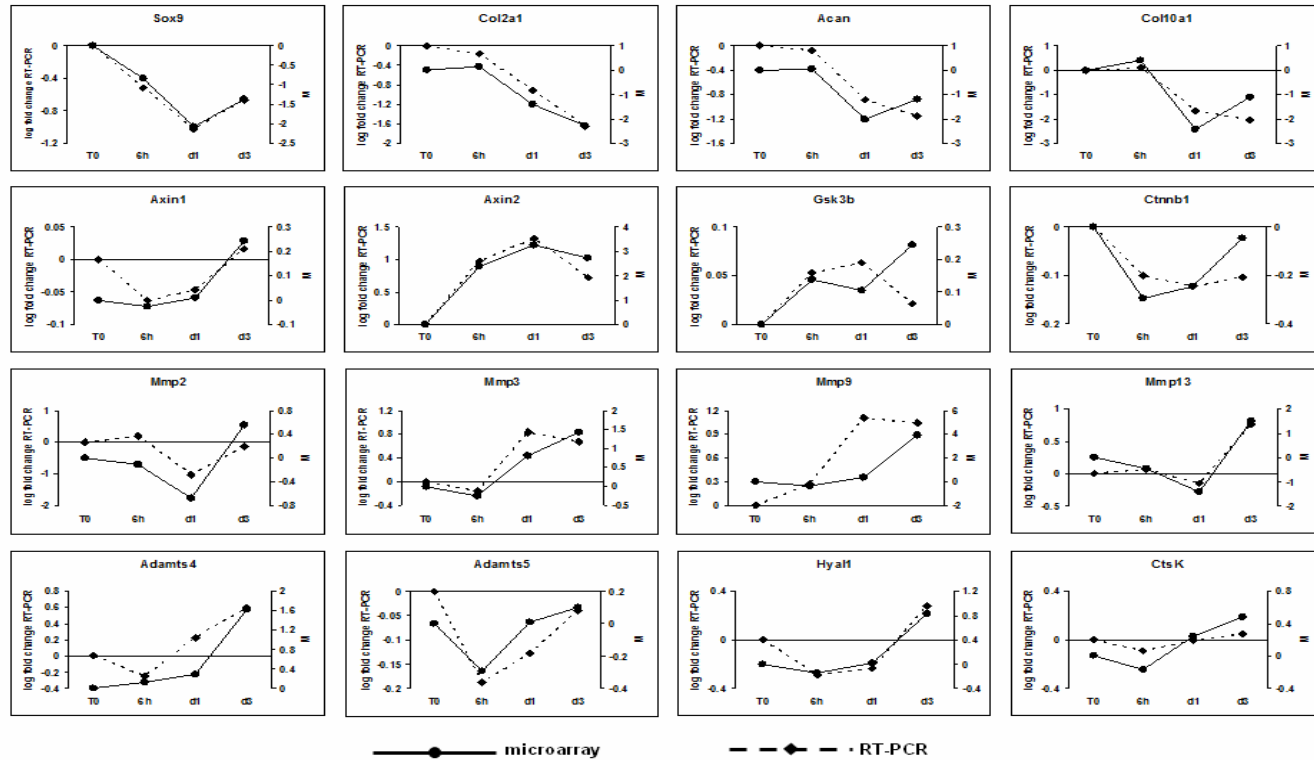


Figure 5. Quantitative Real-Time RT-PCR validates the microarray data. Correlation between qPCR and microarray results for *Sox9*, *Col2a1*, *Acan*, *Col10a1*, *Axin1*, *Axin2*, *Gsk3b*, *Ctnnb1*, *Mmp2*, *Mmp3*, *Mmp9*, *Mmp13*, *Adams4*, *Adams5*, *Hyal1*, and *CtsK*. The primary y-axis (left) indicates the RT-PCR results as normalized fold change on a log-scale. The secondary y-axis (right) indicates the microarray results as the log differential expression ratios (M). Data are expressed as the mean of N = 6 metatarsals (qPCR) and N = 15 metatarsals (microarray).

GIN induces OA-like effects *in vivo*

We next investigated whether GIN can induce the same biological effects in an *in vivo* experimental model. In an initial experiment, we observed 72 hours after GIN injection nuclear translocation of β -catenin in a dose-dependent fashion in rat knee articular chondrocytes, whereas vehicle treatment did not induce a change in β -catenin expression in the control joints (Figure 6A, A_i, B, B_i and data not shown). Virtually all articular chondrocytes treated with the highest GIN concentration (10^{-5} M) showed nuclear β -catenin expression, yet they did not display any morphological changes or alterations of their ECM. We did not detect β -catenin up-regulation in other tissues such as synovium, tendons, or bone at the examined time point, nor evidence of inflammation.

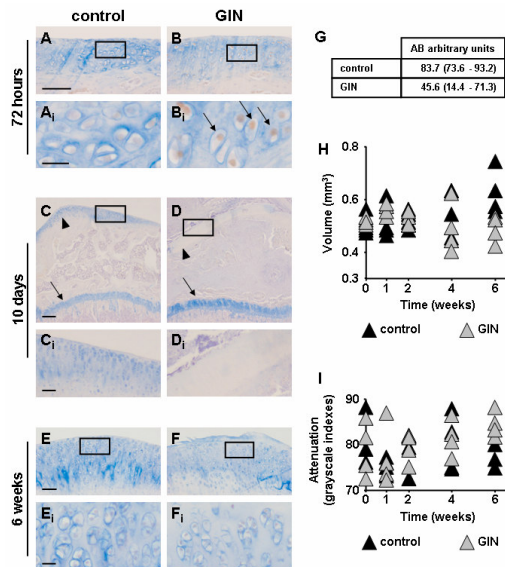


Figure 6. GIN induces OA-like effects in rat articular cartilage. (A, B) Representative pictures of β -catenin IHC combined with AB staining on longitudinal mid-sagittal sections of tibial plateaus 72 hours after injection with vehicle (A) or 10^{-5} M GIN (B). Seventy-two hours after GIN injection there is β -catenin up-regulation (arrows in B_i). (C, D) Representative pictures of AB staining on longitudinal mid-sagittal sections of proximal tibias 10 days after injection with vehicle (C) or 10^{-5} M GIN (D) indicate massive ECM degradation only in the GIN-treated articular cartilage (arrowheads). GP cartilage is unaffected in both conditions (arrows). (E, F) Representative pictures of β -catenin IHC combined with AB staining on longitudinal mid-sagittal sections of tibial plateaus 6 weeks after injection with vehicle (E) or 10^{-5} M GIN (F). Short term GIN treatment does not lead to β -catenin up-regulation 6-weeks-later, but induces OA-like morphological changes of the articular cartilage. (A_i, B_i, C_i, D_i, E_i, F_i) High magnification pictures of the boxed regions in A, B, C, D, E and F, respectively. (G) Quantification of the intensity of the AB staining, at 6 weeks, in the control and GIN-treated knees (N = 4 independent samples) showing less GAGs in the treated samples. Data are expressed as median (range) AB arbitrary units, $p = 0.050$. (H, I) Quantification of volume and attenuation measurements from CECT-data (N = 4 independent samples) (black triangles - controls, grey triangles - GIN treated samples). Scale bars: 200 μ m (A, B, C, D, E, F), 20 μ m (A_i, B_i, E_i, F_i), 300 μ m (C, D).

In a second experiment, we injected 10^{-5} M GIN on day 1, 3 and 5. Four rats (“early” group) displayed signs of severe acute inflammation of the GIN-treated knee beginning at day 7 and these animals were therefore sacrificed already at day 10. No difference in β -catenin expression was observed between the GIN-treated and control knees of these animals (data not shown). In the vehicle-injected knee, the surface of the AC was smooth, the matrix was densely stained with AB and showed no signs of degeneration (Figure 6C, C_i). Besides displaying histological signs of inflammation (intra-articular infiltration of neutrophils and macrophages, synoviocyte hyperplasia, fibrin exudation etc.), the GIN-treated knees in the “early” group displayed intensely degraded AC, containing almost no GAGs, as indicated by absence of AB staining (Figure 6D, D_i and data not shown) in each of the 4 animals.

The other 4 rats (“late” group) from this experiment were sacrificed after 6 weeks and again showed no difference in the β -catenin expression pattern between the GIN-treated knee and controls (Figure 6E, E_i, F, F_i). Whereas no morphological changes were observed in the control knees of the “late” group, GIN-treated samples from all 4 rats displayed superficial fibrillation of AC, focal hypocellularity of chondrocytes, and reduced AB staining. Quantification of the intensity of the AB staining revealed significantly less staining in the cartilage of GIN-treated knees in comparison to contralateral control knees (Figure 6G, $p=0.05$).

Although not statistically significant, CECT analysis of condylar cartilage revealed a trend in reduction of cartilage volume as well as GAG-depletion (expressed by increased attenuation) in the GIN-treated knee joints in comparison to control knees (Figure 6H, I).

DISCUSSION

Here we show that Gsk3 β , by controlling the canonical Wnt signaling pathway, is critical for maintenance of the chondrocytic phenotype. Inhibition of Gsk3 β in chondrocytes *ex vivo* leads to loss of cartilage markers expression, induces matrix degradation by stimulating the expression of Mmps, inhibits chondrocyte proliferation and, most likely as a consequence of these effects, induces chondrocyte apoptosis. In addition, we demonstrate that transient inhibition of Gsk3 β , following three intra-articular injections of GIN in rat knees during 1 week is associated with the appearance of OA-like features 6-weeks later. In agreement with our results, recent findings suggest that upregulation of β -catenin through induction of proteasomal degradation of Gsk3 β in chondrocytes initiates early events of OA, while inhibition of Gsk3 β may block chondrogenesis (20;21).

Besides the canonical Wnt pathway, GSK3 β also regulates signal transduction of the Hedgehog (Hh) and Fibroblast growth factor (Fgf) family of secreted proteins (22;23). Given that both Hh and Fgf growth factors play important roles in the chondrocyte life cycle, we searched in our microarray results for possible target genes of these proteins among the list of transcripts differentially regulated by GIN (24;25). Only PR domain containing 1, with ZNF domain (*Prdm1*) matched this criterion, acting down-

stream of a sequential Wnt and Fgf signaling cascade (26). Our microarray expression data indicated that GIN treatment up-regulated the canonical Wnt target genes *Axin2* and *Apcdd1*, transcripts that have previously been shown to be induced only by Wnt and not by Fgf signaling (27-29). The protein products of *Axin2* and *Naked cuticle homolog 2*, both of which are upregulated in the microarray, are both renowned antagonists of the canonical Wnt signal. They have been shown to participate in negative feedback regulation of β -catenin activity (30-32). Taken together, these findings suggest that the intense cartilage matrix degeneration as well as the loss of the chondrocytic phenotype following GIN treatment occurred, at least in our experimental set-up, mainly due and can be explained by the activation of the Wnt/ β -catenin pathway, although we cannot exclude minor roles of other signaling pathways in which GSK3 β is known to be implicated nor of minor off-target effects of GIN.

Previously, we and others have reported that continuous exposure of chondrocytes to extensive levels of β -catenin *in vivo* induces loss of the chondrocytic phenotype as evidenced by the loss in expression of typical chondrocyte markers (5;6). Microarray analysis of GIN-treated metatarsals confirmed and extended this observation. Furthermore, our microscopical analysis suggests that GIN not only induced an enhanced degradation of the ECM, but also inhibited the expression of several ECM constituents in a time-dependent manner. Noteworthy, in the metatarsal experiments the loss of expression of typical cartilage markers at the mRNA level was observed before protein degradation was noticeable. GIN treatment inhibited the expression of genes encoding collagenous (*Col9a3*, *Col11a1*, and *Col14a1*), and non-collagenous ECM proteins (*Ucma*, *Matn1*, *Matn3*, *Matn4*, *Hapln1*, *Fmod*, *Mgp*), as well as proteoglycans (*Epyc*). In addition, GIN stimulated the expression of proteinases *Mmp9*, *Mmp10*, *Mmp11*, and *Htra1*, which promote ECM degradation, suggesting that the loss of tissue integrity observed in the treated metatarsals is due not only to a loss of the links between the collagenous and the non-collagenous proteins in the matrix, but also to active matrix degradation.

Decreased chondrocyte proliferation, augmented apoptosis, loss of the chondrocytic phenotype and degradation of ECM together characterize the “degradative phase” of OA, the most common form of arthritis (33). These pathological phenomena were observed after up-regulated canonical Wnt signaling by GIN-treatment in our experimental set-ups *ex vivo* and *in vivo*, in agreement with recent data suggesting a link between excess signaling through the Wnt/ β -catenin pathway and OA (6). Moreover, many genes reportedly induced in OA cartilage were up-regulated by GIN treatment: *Mmp9*, *Mmp10*, *Mmp11*, *Axin2*, *Htra1*, angiopoietin-like 2 (*Angptl2*), and met proto-oncogene (*Met*) (2;34-38). *Htra1*, which is increased several-fold in joint cartilage of OA patients, promotes degeneration of cartilage (36;39), while *Met*, besides contributing to the altered metabolism during OA, also stimulates osteophyte development (40). *Serping1*, previously reported to be repressed in OA, and *Matn3*, whose inactivation leads to higher incidence of OA, were both down-regulated by GIN (41;42). In addition, inactivation of *Frzb*, another transcript repressed by GIN treatment, renders joints more susceptible for osteoarthritic changes (43).

Our results suggest that treatment with GIN can induce cartilage degeneration of rat AC after 3 intra-articular injections of GIN with a two days interval. We observed two distinct phenotypes, most likely explained by a difference in retention time of GIN

in the knee joint: a severe form with acute inflammation associated with resorption already 10 days after the first injection a milder phenotype. The potent catabolic effects of GIN on cartilage may have caused rapid and excessive cartilage degradation. These degradation products may have triggered an acute form of inflammation through the release of for example collagen type II fragments. In animals with the milder phenotype, microscopical analysis demonstrated the presence of the first signs of OA-like changes such as surface fibrillation, focal chondrocyte hypocellularity and a decrease in GAG staining in GIN-treated knees but not in the contralateral control knees 6-weeks after the last GIN-injection. CECT analysis revealed a trend of less cartilage volume and more attenuation, indicative for GAG loss in the GIN treated animals; however this observation did not reach significance. In contrast to the increased β -catenin expression in AC present 3 days after GIN injection, we did not detect increased β -catenin staining 6 weeks after GIN injection nor did we find evidence for nuclear β -catenin accumulation in the synovium, tendons or bone at each of the analysed time points. This suggests that a transient rise in β -catenin in AC may be sufficient to trigger development of OA-like features, an observation that extends findings in conditional constitutive mice carrying a stabilized, oncogenic variant of β -catenin, which also develop OA (4). Although we did not find evidence for increased β -catenin accumulation in other joint tissues besides cartilage at the examined time points, we cannot exclude that GIN-injection has resulted in a more rapid and transient rise of β -catenin in these tissues which was normalized 72 hours after the injection. This may have also contributed to the observed pathology. Furthermore, we cannot exclude that the mild cartilage phenotype was due to a milder form of inflammation in the first weeks after injection. However, given the clear evidence of increased nuclear β -catenin accumulation in AC 72 hours after GIN injection and the consistency of the *in vivo* findings with the phenotypic changes and effects on gene expression of GIN in our *ex vivo* cartilage explant model, we favor the hypothesis that these first indications of cartilage degeneration were due to a transient rise in β -catenin in AC triggering cartilage catabolism and changes in the chondrocyte phenotype.

Abnormally regulated GSK3 β has been associated with many pathological conditions like Alzheimer's disease, mood disorders, diabetes and cancer (7). However, a direct link between GSK3 β and the pathophysiology of OA has not yet been reported. Since in our experimental set-ups the GIN-induced effects reflect some of the pathological findings normally seen in osteoarthritic chondrocytes, we speculate that Gsk3 β plays a role in the pathophysiology of this degenerative cartilage disease as well, most likely by regulating the levels of β -catenin. Whether pharmacological modulation of Gsk3 β might represent a potential novel therapeutical approach for the management of OA remains to be elucidated.

ACKNOWLEDGEMENTS

This work was financially supported by an unrestricted educational grant from IP-SEN FARMACEUTICA BV to RLM that we gratefully acknowledge.

CONTRIBUTIONS

Conception and design: RLM, MK; Collection of data: RLM, MS; Analysis and interpretation of the data: RLM, MS, LF, JIG, HW, JMW, ECR-M, MK; Drafting of the article: RLM; Critical revision of the article for important intellectual content: RLM, MS, LF, JIG, CWL, WO, HW, JMW, ECR-M, MK; Final approval of the article: RLM, MS, LF, JIG, CWL, WO, HW, JMW, ECR-M, MK; Statistical expertise: LF, JIG.

Table 1. List of GIN-down-regulated genes identified by PCA with a minimal fold change < -2.

Gene symbol	Affymetrix code	Fold change
Adipoq	1422651_at	-5.14
Ucma	1428994_s_at	-4.74
Cxcl5	1419728_at	-4.32
Chrdl1	1434201_at	-4.27
Abi3bp	1427053_at	-4.13
Cytl1	1456793_at	-3.99
Ecrq4	1460049_s_at	-3.96
G0s2	1448700_at	-3.86
Srpx	1451939_a_at	-3.83
Abi3bp	1427054_s_at	-3.82
Mia1	1419608_a_at	-3.79
Cfd	1417867_at	-3.75
Islr	1418450_at	-3.67
Frzb	1416658_at	-3.65
Omd	1418745_at	-3.63
Ecrq4	1423261_at	-3.63
Ogn	1419662_at	-3.58
Frzb	1448424_at	-3.56
Ucma	1428993_at	-3.51
Cyp7b1	1421074_at	-3.42
Depdc6	1451348_at	-3.42
Ogn	1419663_at	-3.36
Hp	1448881_at	-3.25
Lpl	1431056_a_at	-3.23
Wwp2	1456714_at	-3.21
Pdcd4	1418840_at	-3.18
Penk1	1427038_at	-3.12
Lcn2	1427747_a_at	-3.11
Ptx3	1418666_at	-3.11
Angptl1	1455224_at	-3.09
Steap4	1460197_a_at	-3.09
Angpt1	1439066_at	-3.08
Calml4	1424713_at	-3.07
Lect1	1460258_at	-3.05
Lpl	1415904_at	-3.04
Matn1	1418477_at	-3.02
Susd5	1437387_at	-3.02
Hapln1	1421633_a_at	-2.99
Fgf7	1438405_at	-2.96
Mettl7a1	1434150_a_at	-2.96
Chrdl1	1421295_at	-2.96
Wwp2	1457499_at	-2.95

Hapln1	1426294_at	-2.93
5033414K04Rik	1436999_at	-2.92
Prlr	1441102_at	-2.92
Pdcd4	1456393_at	-2.92
Hapln1	1426295_at	-2.9
Sdpr	1416779_at	-2.9
Scin	1450276_a_at	-2.89
Plscr2	1448961_at	-2.85
Cxcl14	1418457_at	-2.85
BB144871	1436453_at	-2.85
Depdc6	1428622_at	-2.81
Mfap4	1424010_at	-2.81
Cyp7b1	1421075_s_at	-2.8
Matn3	1422148_at	-2.79
Gas2	1450112_a_at	-2.77
Depdc6	1443579_s_at	-2.76
6330403K07Rik	1426766_at	-2.76
Rspo3	1455607_at	-2.76
Al646023	1456878_at	-2.75
Mup1	1420465_s_at	-2.73
Col11a1	1449154_at	-2.73
Wwp2	1438482_at	-2.73
Efcab1	1455074_at	-2.72
Peg3	1417356_at	-2.7
Prlr	1448556_at	-2.7
Wwp2	1448145_at	-2.69
Meg3	1436713_s_at	-2.69
Vcam1	1448162_at	-2.67
Scara5	1451204_at	-2.67
Chrdl1	1456722_at	-2.66
Prlr	1437397_at	-2.63
Vnn1	1418486_at	-2.63
Lbp	1448550_at	-2.62
Peg3	1417355_at	-2.62
Agtr1a	1436739_at	-2.61
Adhfe1	1424393_s_at	-2.6
Pdlim2	1423946_at	-2.58
S100b	1434342_at	-2.58
Fxyd3	1418374_at	-2.56
Rora	1457177_at	-2.56
Hapln1	1438020_at	-2.54
Rian	1428055_at	-2.53
Slc1a3	1426340_at	-2.52
Ppp1r3c	1433691_at	-2.52
Fry	1456480_at	-2.51

Gsk3 β inhibition promotes cartilage degradation

Sorbs2	1437197_at	-2.5
Meg3	1452905_at	-2.5
Matn4	1418464_at	-2.5
Scrg1	1420764_at	-2.49
Hapln1	1458109_at	-2.48
Meg3	1428764_at	-2.47
Gda	1435748_at	-2.47
Fibin	1419376_at	-2.47
Cmtm5	1430600_at	-2.47
Mgp	1448416_at	-2.47
Kcnt2	1459971_at	-2.46
Angpt1	1421421_at	-2.46
Nope	1416474_at	-2.46
Kcnt2	1440030_at	-2.46
Sdpr	1416778_at	-2.43
Angpt1	1421441_at	-2.43
Efcab1	1454198_a_at	-2.42
Epyc	1421114_a_at	-2.42
Wwp2	1448146_at	-2.41
Gpr27	1434848_at	-2.41
Zim1	1421405_at	-2.4
Matn3	1455948_x_at	-2.39
Mup3	1426154_s_at	-2.39
Sec16b	1450734_at	-2.38
Epha3	1455426_at	-2.37
Sema3d	1453148_at	-2.37
Fmod	1437685_x_at	-2.36
Hhip	1421426_at	-2.36
Tox	1425483_at	-2.36
Pak3	1435486_at	-2.35
Car3	1449434_at	-2.35
1110006E14Rik	1431094_at	-2.35
Sdr39u1	1459269_at	-2.35
Fgf7	1422243_at	-2.35
Hcfc1r1	1428406_s_at	-2.34
Copg2	1445268_at	-2.34
Msr1	1448061_at	-2.34
Fmod	1456084_x_at	-2.33
Sorbs2	1441624_at	-2.32
Clec11a	1418796_at	-2.32
S3-12	1418595_at	-2.32
Prlr	1425853_s_at	-2.31
Peg3	1433924_at	-2.31
Ly6c1	1421571_a_at	-2.31
Car3	1460256_at	-2.31

Gnas	1444767_at	-2.29
Col14a1	1427168_a_at	-2.28
Ifi27	1426278_at	-2.28
Afap1l2	1436870_s_at	-2.28
Depdc6	1453571_at	-2.27
Mfap5	1418454_at	-2.27
Aldh6a1	1448104_at	-2.27
Sdpr	1443832_s_at	-2.26
Papola	1419032_at	-2.26
Kctd4	1420537_at	-2.25
Papss2	1421989_s_at	-2.25
Aff3	1433939_at	-2.24
Cxcl1	1419209_at	-2.24
Fzd4	1419301_at	-2.23
Rnf144b	1439153_at	-2.23
Pparg	1420715_a_at	-2.23
Rarres2	1428538_s_at	-2.22
Serping1	1416625_at	-2.22
C3	1423954_at	-2.21
Lilrb4	1420394_s_at	-2.21
Rspo2	1455893_at	-2.21
Tnmd	1417979_at	-2.21
Csgalnact1	1452365_at	-2.2
Maf	1447849_s_at	-2.2
Aspn	1416652_at	-2.2
Rgs5	1417466_at	-2.2
Fmod	1415939_at	-2.2
6530401D17Rik	1451679_at	-2.2
Pak3	1437318_at	-2.19
Efemp1	1427183_at	-2.18
Cybrd1	1460604_at	-2.18
Olfml1	1455663_at	-2.18
Fmod	1437718_x_at	-2.18
Gtl2	1429257_at	-2.18
9530019H20Rik	1458113_at	-2.17
Scara3	1427020_at	-2.17
Zfpm2	1449314_at	-2.17
Pira6	1420464_s_at	-2.17
Crispld1	1423352_at	-2.17
Papss2	1421987_at	-2.17
Cxcl12	1448823_at	-2.17
Susd5	1438636_s_at	-2.17
S100b	1419383_at	-2.16
Klhl24	1451793_at	-2.16
Ptgis	1448816_at	-2.15

Nope	1416473_a_at	-2.15
Akr1c14	1418979_at	-2.15
Hs6st2	1450047_at	-2.15
Tox	1446950_at	-2.15
2310050P20Rik	1453841_at	-2.14
Mest	1423294_at	-2.14
Hcfc1r1	1428405_at	-2.14
Mettl7a1	1454858_x_at	-2.14
Mirg	1457030_at	-2.13
Mme	1455961_at	-2.12
N4bp2l1	1417707_at	-2.12
Lcp1	1415983_at	-2.12
B230217C12Rik	1428568_at	-2.12
Ccl9	1417936_at	-2.12
Agtr2	1415832_at	-2.12
Ccl9	1448898_at	-2.11
Ptprc	1422124_a_at	-2.11
Meg3	1428765_at	-2.1
Gda	1435749_at	-2.1
Itgbl1	1425039_at	-2.1
Gstt1	1418186_at	-2.1
Hhip	1437933_at	-2.09
Mettl7a1	1434151_at	-2.08
Apoc1	1417561_at	-2.08
Itih5	1429159_at	-2.08
Papola	1419033_at	-2.08
Lrrc17	1429679_at	-2.07
Aff3	1441172_at	-2.06
LOC552901	1458505_at	-2.06
Fxyd1	1421374_a_at	-2.06
Smoc2	1431362_a_at	-2.06
Fgfr3	1421841_at	-2.06
Vkorc1	1452770_at	-2.06
Meg3	1429256_at	-2.05
Klhl24	1438519_at	-2.05
Col9a3	1460693_a_at	-2.04
Epha3	1425575_at	-2.04
Ttc30b	1423672_at	-2.04
AI449310	1455452_x_at	-2.03
Mme	1422975_at	-2.03
Tox	1445612_at	-2.02
Ctgf	1416953_at	-2.02
Col11a1	1418599_at	-2.02
Ebf3	1460666_a_at	-2.02
Mxd4	1434378_a_at	-2.01

Chapter 6

Arhgap20	1429918_at	-2.01
Lsp1	1417756_a_at	-2.01
Fbln7	1460412_at	-2.01

Table 2. List of GIN-up-regulated genes identified by PCA with a minimal fold change > +2.

Gene symbol	Affymetrix code	Fold change
Cadps	1448955_s_at	4.55
Mmp10	1420450_at	4.44
Dsp	1435494_s_at	4.42
Dsp	1435493_at	4.26
Ened	1429637_at	4.02
Inhbb	1426858_at	3.72
Ened	1416805_at	3.67
Mmp11	1417234_at	3.61
Apcdd1	1454822_x_at	3.5
1810011O10Rik	1435595_at	3.47
Prdm1	1420425_at	3.45
Snca	1436853_a_at	3.44
Il11	1449982_at	3.43
Apcdd1	1449070_x_at	3.41
Nkd2	1434275_at	3.38
LOC624112	1440815_x_at	3.25
Apcdd1	1418382_at	3.25
1810011O10Rik	1451415_at	3.19
Cadps	1444488_at	3.17
Axin2	1436845_at	3.09
Adcy1	1456487_at	3.08
Plekhg4	1457145_at	3.06
Nkd2	1419466_at	3.06
Krt39	1437440_at	3.03
Fhod3	1435551_at	2.93
Tmem8	1418344_at	2.92
Sema4f	1439768_x_at	2.91
Snca	1418493_a_at	2.84
Apcdd1	1418383_at	2.83
4921509J17Rik	1429106_at	2.8
Cxcr6	1425832_a_at	2.77
Nkd2	1419465_at	2.75
Myh1	1427868_x_at	2.74
Ccl8	1419684_at	2.73
Cps1	1455540_at	2.71
Notum	1451857_a_at	2.71
Gnai1	1454959_s_at	2.69
4921509J17Rik	1439093_at	2.66
Htr2b	1422125_at	2.61
Gnai1	1434440_at	2.61
Met	1434447_at	2.6
Mmp9	1448291_at	2.46

Myh1	1427520_a_at	2.46
Ccbe1	1437385_at	2.46
Mmp9	1416298_at	2.45
Ndp	1449251_at	2.43
Cadps	1458298_at	2.42
Rcan1	1416600_a_at	2.4
Stmn4	1418105_at	2.38
Twist2	1448925_at	2.37
Hspa4l	1418253_a_at	2.34
Ampd3	1422573_at	2.34
Rcan1	1416601_a_at	2.31
Cxcr6	1422812_at	2.3
Htra1	1438251_x_at	2.3
Tec	1460204_at	2.28
Mafb	1451715_at	2.27
Angptl2	1455090_at	2.27
Angptl2	1421002_at	2.26
Tnc	1456344_at	2.25
Masp1	1425985_s_at	2.25
Angptl2	1450085_at	2.23
Mafb	1451716_at	2.22
Krt19	1417156_at	2.21
Msc	1418417_at	2.21
Arl4c	1454788_at	2.21
Htra1	1416749_at	2.2
Ankrd1	1420992_at	2.19
Dio2	1418937_at	2.18
Cryab	1434369_a_at	2.17
AI425999	1435657_at	2.16
Gsta2	1421040_a_at	2.16
2210408K08Rik	1437087_at	2.15
Cryab	1416455_a_at	2.15
Ppargc1a	1434099_at	2.11
Gnai1	1427510_at	2.1
Pla2g7	1430700_a_at	2.09
2310076G05Rik	1442077_at	2.09
Pmepa1	1452295_at	2.07
Gsta2	1421041_s_at	2.07
Bex1	1448595_a_at	2.06
Ppargc1a	1456395_at	2.05
4631422O05Rik	1428861_at	2.05
Chst1	1449147_at	2.05
Vash2	1451105_at	2.04
Hspa4l	1458385_at	2.04
Ankrd1	1420991_at	2.04

Gsk3 β inhibition promotes cartilage degradation

Lcp2	1418641_at	2.03
Slco5a1	1440874_at	2.03
Hmgn3	1459040_at	2.02
Mex3b	1437152_at	2.02

REFERENCES

1. Pacifici M, Koyama E, Iwamoto M. Mechanisms of synovial joint and articular cartilage formation: recent advances, but many lingering mysteries. *Birth Defects Res C Embryo Today* 2005; 75(3):237-48.
2. Aigner T, Zien A, Gehrsitz A, Gebhard PM, McKenna L. Anabolic and catabolic gene expression pattern analysis in normal versus osteoarthritic cartilage using complementary DNA-array technology. *Arthritis Rheum* 2001; 44(12):2777-89.
3. Zhu M, Chen M, Zuscik M, Wu Q, Wang YJ, Rosier RN et al. Inhibition of beta-catenin signaling in articular chondrocytes results in articular cartilage destruction. *Arthritis Rheum* 2008; 58(7):2053-64.
4. Zhu M, Tang D, Wu Q, Hao S, Chen M, Xie C et al. Activation of beta-catenin signaling in articular chondrocytes leads to osteoarthritis-like phenotype in adult beta-catenin conditional activation mice. *J Bone Miner Res* 2009; 24(1):12-21.
5. Miclea RL, Karperien M, Bosch CA, van der Horst G, van der Valk MA, Kobayashi T et al. Adenomatous polyposis coli-mediated control of beta-catenin is essential for both chondrogenic and osteogenic differentiation of skeletal precursors. *BMC Dev Biol* 2009; 9(1):26.
6. Chun JS, Oh H, Yang S, Park M. Wnt signaling in cartilage development and degeneration. *BMB Rep* 2008; 41(7):485-94.
7. Doble BW, Woodgett JR. GSK-3: tricks of the trade for a multi-tasking kinase. *J Cell Sci* 2003; 116(Pt 7):1175-86.
8. Kapadia RM, Guntur AR, Reinhold MI, Naski MC. Glycogen synthase kinase 3 controls endochondral bone development: contribution of fibroblast growth factor 18. *Dev Biol* 2005; 285(2):496-507.
9. Engler TA, Henry JR, Malhotra S, Cunningham B, Furness K, Brozinick J et al. Substituted 3-imidazo[1,2-a]pyridin-3-yl- 4-(1,2,3,4-tetrahydro-[1,4]diazepino-[6,7,1-hi]indol-7-yl)pyrrole-2,5-diones as highly selective and potent inhibitors of glycogen synthase kinase-3. *J Med Chem* 2004; 47(16):3934-7.
10. van der Horst G, van der Werf SM, Farih-Sips H, van Bezooijen RL, Lowik CW, Karperien M. Downregulation of Wnt signaling by increased expression of Dickkopf-1 and -2 is a prerequisite for late-stage osteoblast differentiation of KS483 cells. *J Bone Miner Res* 2005; 20(10):1867-77.
11. Smink JJ, Buchholz IM, Hamers N, van Tilburg CM, Christis C, Sakkars RJ et al. Short-term glucocorticoid treatment of piglets causes changes in growth plate morphology and angiogenesis. *Osteoarthritis Cartilage* 2003; 11(12):864-71.
12. Hoogendam J, Parlevliet E, Miclea R, Lowik CW, Wit JM, Karperien M. Novel early target genes of parathyroid hormone-related peptide in chondrocytes. *Endocrinology* 2006; 147(6):3141-52.
13. Jonnalagadda S, Srinivasan R. Principal components analysis based methodology to identify differentially expressed genes in time-course microarray data. *BMC Bioinformatics* 2008; 9:267.

14. Huang da W, Sherman BT, Lempicki RA. Systematic and integrative analysis of large gene lists using DAVID bioinformatics resources. *Nat Protoc* 2009; 4(1):44-57.
15. Dennis G, Jr., Sherman BT, Hosack DA, Yang J, Gao W, Lane HC et al. DAVID: Database for Annotation, Visualization, and Integrated Discovery. *Genome Biol* 2003; 4(5):3.
16. Ashburner M, Ball CA, Blake JA, Botstein D, Butler H, Cherry JM et al. Gene ontology: tool for the unification of biology. The Gene Ontology Consortium. *Nat Genet* 2000; 25(1):25-9.
17. Palmer AW, Guldberg RE, Levenston ME. Analysis of cartilage matrix fixed charge density and three-dimensional morphology via contrast-enhanced microcomputed tomography. *Proc Natl Acad Sci U S A* 2006; 103(51):19255-60.
18. Cai Y, Mohseny AB, Karperien M, Hogendoorn PC, Zhou G, Cleton-Jansen AM. Inactive Wnt/beta-catenin pathway in conventional high-grade osteosarcoma. *J Pathol* 2010; 220(1):24-33.
19. Mushtaq T, Bijman P, Ahmed SF, Farquharson C. Insulin-like growth factor-I augments chondrocyte hypertrophy and reverses glucocorticoid-mediated growth retardation in fetal mice metatarsal cultures. *Endocrinology* 2004; 145(5):2478-86.
20. Wu Q, Huang JH, Sampson ER, Kim KO, Zuscik MJ, O'Keefe RJ et al. Smurf2 induces degradation of GSK-3beta and upregulates beta-catenin in chondrocytes: a potential mechanism for Smurf2-induced degeneration of articular cartilage. *Exp Cell Res* 2009; 315(14):2386-98.
21. Choi YA, Kang SS, Jin EJ. BMP-2 treatment of C3H10T1/2 mesenchymal cells blocks MMP-9 activity during chondrocyte commitment. *Cell Biol Int* 2009; 33(8):887-92.
22. Takenaka K, Kise Y, Miki H. GSK3beta positively regulates Hedgehog signaling through Sufu in mammalian cells. *Biochem Biophys Res Commun* 2007; 353(2):501-8.
23. Katoh M, Katoh M. Cross-talk of WNT and FGF signaling pathways at GSK3beta to regulate beta-catenin and SNAIL signaling cascades. *Cancer Biol Ther* 2006; 5(9):1059-64.
24. Day TF, Yang Y. Wnt and hedgehog signaling pathways in bone development. *J Bone Joint Surg Am* 2008; 90 Suppl 1:19-24.
25. Ornitz DM. FGF signaling in the developing endochondral skeleton. *Cytokine Growth Factor Rev* 2005; 16(2):205-13.
26. Mercader N, Fischer S, Neumann CJ. Prdm1 acts downstream of a sequential RA, Wnt and Fgf signaling cascade during zebrafish forelimb induction. *Development* 2006; 133(15):2805-15.
27. ten Berge D, Brugmann SA, Helms JA, Nusse R. Wnt and FGF signals interact to coordinate growth with cell fate specification during limb development. *Development* 2008; 135(19):3247-57.
28. Rousset R, Mack JA, Wharton KA, Jr., Axelrod JD, Cadigan KM, Fish MP et al. Naked cuticle targets dishevelled to antagonize Wnt signal transduction. *Genes Dev* 2001; 15(6):658-71.
29. Jukkola T, Sinjushina N, Partanen J. Drapc1 expression during mouse embryonic development. *Gene Expr Patterns* 2004; 4(6):755-62.
30. Zeng W, Wharton KA, Jr., Mack JA, Wang K, Gadbow M, Suyama K et al. naked cuticle encodes an inducible antagonist of Wnt signalling. *Nature* 2000; 403(6771):789-95.
31. Moon RT, Bowerman B, Boutros M, Perrimon N. The promise and perils of Wnt signaling through beta-catenin. *Science* 2002; 296(5573):1644-6.

32. Jho EH, Zhang T, Domon C, Joo CK, Freund JN, Costantini F. Wnt/beta-catenin/Tcf signaling induces the transcription of Axin2, a negative regulator of the signaling pathway. *Mol Cell Biol* 2002; 22(4):1172-83.
33. Sandell LJ, Aigner T. Articular cartilage and changes in arthritis. An introduction: cell biology of osteoarthritis. *Arthritis Res* 2001; 3(2):107-13.
34. Mohtai M, Smith RL, Schurman DJ, Tsuji Y, Torti FM, Hutchinson NI et al. Expression of 92-kD type IV collagenase/gelatinase (gelatinase B) in osteoarthritic cartilage and its induction in normal human articular cartilage by interleukin 1. *J Clin Invest* 1993; 92(1):179-85.
35. Pfander D, Cramer T, Weseloh G, Pullig O, Schuppan D, Bauer M et al. Hepatocyte growth factor in human osteoarthritic cartilage. *Osteoarthritis Cartilage* 1999; 7(6):548-59.
36. Tsuchiya A, Yano M, Tocharus J, Kojima H, Fukumoto M, Kawaichi M et al. Expression of mouse HtrA1 serine protease in normal bone and cartilage and its upregulation in joint cartilage damaged by experimental arthritis. *Bone* 2005; 37(3):323-36.
37. Meng J, Ma X, Ma D, Xu C. Microarray analysis of differential gene expression in temporomandibular joint condylar cartilage after experimentally induced osteoarthritis. *Osteoarthritis Cartilage* 2005; 13(12):1115-25.
38. Velasco J, Zarrabeitia MT, Prieto JR, Perez-Castrillon JL, Perez-Aguilar MD, Perez-Nunez MI et al. Wnt pathway genes in osteoporosis and osteoarthritis: differential expression and genetic association study. *Osteoporos Int* 2009.
39. Hu SI, Carozza M, Klein M, Nantermet P, Luk D, Crowl RM. Human HtrA, an evolutionarily conserved serine protease identified as a differentially expressed gene product in osteoarthritic cartilage. *J Biol Chem* 1998; 273(51):34406-12.
40. Dankbar B, Neugebauer K, Wunrau C, Tibesku CO, Skwara A, Pap T et al. Hepatocyte growth factor induction of macrophage chemoattractant protein-1 and osteophyte-inducing factors in osteoarthritis. *J Orthop Res* 2007; 25(5):569-77.
41. van der Weyden L, Wei L, Luo J, Yang X, Birk DE, Adams DJ et al. Functional knockout of the matrilin-3 gene causes premature chondrocyte maturation to hypertrophy and increases bone mineral density and osteoarthritis. *Am J Pathol* 2006; 169(2):515-27.
42. Gebauer M, Saas J, Haag J, Dietz U, Takigawa M, Bartnik E et al. Repression of anti-proliferative factor Tob1 in osteoarthritic cartilage. *Arthritis Res Ther* 2005; 7(2):R274-R284.
43. Lories RJ, Peeters J, Bakker A, Tylzanowski P, Derese I, Schrooten J et al. Articular cartilage and biomechanical properties of the long bones in Frzb-knockout mice. *Arthritis Rheum* 2007; 56(12):4095-103.